

# Using Metar - Data to Calculate In-Cloud Icing on a Mountain Site near by the Airport

Dr. K. Harstveit

Kjeller Vindteknikk

Po 122, 2027 Kjeller, Norway, [knut.harsveit@vindteknikk.no](mailto:knut.harsveit@vindteknikk.no)

**Abstract—** In the cold season, in-cloud rime were calculated at reference object on mountain tops by an ice accretion model, and an energy balance equation modified to allow for ice shedding. Air temperature and wind speed were observed at the icing site, and compared to extrapolated data from a representative airport or a high-quality automatic weather station. Cloud observations were taken from metar-data from the airport. The water vapour pressure was assumed to be saturated at cloud base. A shedding factor is defined as a speed-up factor of the ice melting due to ice fall off during positive air temperatures.

When the icing site was situated above cloud base, the liquid water content was assumed to be proportional to the condensation water calculated from the adiabatic saturation curve. For temperatures below 0°C, the cloud droplets were assumed to be liquid and freeze when hitting an object. The modelled ice amounts were compared to observations from two exposed mountain sites on the western coast of Norway; Gamlemsveten (790 masl.) close to Ålesund airport, and Bråsviksåta (723 masl.) close to Bergen, and Deadwater Fell (580 masl.) at the border between England and Scotland. Also made are ice calculations by data from Bodø airport for a recently power line damage at an exposed mountain site in Steigen (385 masl.) at the coast of northern Norway. When allowing for a shedding factor,  $sh=10$ , there was a nice coincidence between observations and modelled ice weights

## I. INTRODUCTION

IN-cloud icing on power lines and telecommunication structures in cold regions is a well identified problem. There is also an increasing need for ice information on wind turbines in such regions. When a structure is situated at a mountainous site above cloud base, super cooled droplets at low temperatures will hit the object, and ice will form on the structure. Such type of icing is also well-known at aeroplanes crossing low clouds in cold regions.

The process is accelerated in strong wind, or relative air speed for moving objects, and increases with increasing super cooled water content in the cloud. Large droplets more easily hit the object, and the number of hits increases with the wind speed. All those parameters usually increase with height, but for increasing mountain height within a given area, the increase in liquid water due to humid air masses lifted above the mountain is the far most effective height effect.

The icing also increases with the object cross section, though strongly modified through increasing deflection of the droplets.

The ice accretion process is fair described in ISO 12494, 2000 [1], build on earlier work, see for instance Makkonen, 1984 [2], Makkonen and Stallabrass, 1987 [3], Finstad et. al

1988 [4], [5]. Ahti and Makkonen, 1995 [6] modelled the ice accretion by using the wind speed dependency in cloudy weather and typical supercooled temperature interval (-15 – 0°C). The wind speed function was found from measurements of wind speed and icing at Pyhäyunturi (477 m asl in Finland).

Harstveit, 2002 [7] has shown the possibility of modelling the ice by the full accretion theory for exposed sites from metar data from a representative airport by presuming adiabatic cloud water gradient. In this paper, the model will be further refined and validated by using data from Gamlemsveten 793 masl, and Brossviksåta, 723 masl, Western Norway, and Deadwater Fell, 580 masl at the boarder of England and Scotland. At those three sites, icing data exists. The model is also tested for a power line break down episode at Steigen, 385 masl, Northern Norway. All sites are exposed for moist maritime air masses.

## II. METHODS AND CALCULATIONS

### A. Model Description

The object exposed to in-cloud icing is presumed to be well inside the cloud. The ice accumulation model described in [1]

$$\frac{dM}{dt} = \alpha_1 \alpha_2 \alpha_3 \cdot w \cdot A \cdot V \quad (1)$$

is used. When super cooled cloud droplets hit the object, the droplets freeze. The ice accretion increases with the liquid water content,  $w$ , the wind speed,  $V$  and the cross section  $A$  of the object. However, not all the droplets hit the object. Small droplets, large objects and low wind speed reduce the hit through the collision coefficient,  $\alpha_1 \leq 1.0$ . Generally, not all the droplets hitting the object, stick to the object, the sticking coefficient,  $\alpha_2 \leq 1.0$ . At temperatures not far from zero, the energy released from the super cooled droplets when freezing at the surface, may be higher than the energy loss from the surface, where the sensible and latent heat are the main contributors. Some of the water will not freeze, but blow off, an effect entering the model through the accretion coefficient,  $\alpha_3 \leq 1.0$ .

For actual atmospheric conditions during in-cloud icing,  $\alpha_1 \approx \alpha_1(V, d, A)$ ;  $\alpha_2 = 1.0$ ;  $\alpha_3 \approx \alpha_3(V, d, A, T_w, e_a(T_d))$ , where  $V$  is the wind speed,  $d$  the droplet diameter,  $A$  the object cross section,  $T_a$  the temperature and  $e_a$  the vapour pressure curve at

$T_a$ . For the complete mathematical expression of the  $\alpha_i$  – coefficients, it is referred to [1]. The model is based on slender, cylindrical objects. For thick objects, or heavily iced object of all kinds, the collision theory breaks down [3]. For ice weights exceeding some 15 – 30 kg/m, dependent on droplet size and wind speed, the collision theory is not longer valid. This does not seriously affect the calculations made here, since the ice weights are smaller, and only for the highest peak weight at the mountain top Gamlemsveten some inaccuracies are introduced.

To calculate the ice accretion during in-cloud icing according to (1), we need the information of the wind speed,  $V$ , the air temperature,  $T_a$ , the liquid cloud water,  $w$ , and the diameter of the cloud droplets,  $d$ . We assume that the icing occur on a rotating cylinder with diameter 0.03 m, and follow the specifications given in [1]. Then cylindrical ice is build up, and the cross section,  $A$  is updated hourly.

$T_a$  and  $V$  is either measured on the site or modelled from high quality routine weather stations. At those stations,  $T_0$ ,  $V_0$ , cloud cover and cloud amount are measured every hour. When high quality site temperatures are missing,  $T_a$ , is calculated using the gradients given in [7]. The wind speed is calculated using the exponential wind formulae;

$$\frac{V(z_{WS})}{V(10)} = \left( \frac{z_{WS}}{10} \right)^n \quad (2)$$

where  $Z_{WS}$  is height above routine weather station level. If no information of the wind speed exists (Steigen), the technique described in [7] is used, by comparing wind data climatology from the closest atmospheric sounding station to the data from the routine weather station. If reliable values exist, but not during icing conditions, the exponent,  $n$  is calculated by comparing wind observations at the routine station to the site station during reliable data periods (Brossviksåta, Deadwater fell).

Above cloud base, the water content may be assumed to be proportional to the adiabatic cloud water gradient and the height above cloud base:

$$w = \alpha \delta (z - H_C) \quad (3)$$

where  $\alpha \approx 1$  or slightly less [8], [9], and [10].  $\alpha < 1$  reflects deviation from the adiabatic cloud water gradient. In [11] there was found  $\alpha = 0.5 - 0.6$  at a hill in a wooded area in Central Finland. From an Amble – diagram, we can presume, at the lowest 500 m of the atmosphere:

$$\delta = 1.56(1 + 0.034\theta_w) \quad [mg\ m^{-4}] \quad (4)$$

where  $\theta_w$  is the potential wet-bulb temperature in °C. The equation expresses the water vapour process of condensation when moist air masses are lifted above lifting condensation level.  $\theta_w$  is calculated from temperature and cloud data.

In the adiabatic process of humid air lifting above the mountain site, condensation starts at the lifting condensation level (LCL), defining the cloud base. Condensation then starts

on the condensation nuclei, and for the quick process at an exposed mountain, the number of droplets is assumed constant, meaning droplet growth during the lifting process. This may be accepted some height above ground, and some height well below the top of the cloud [12]. Close to the ground, droplets are intercepted and this process reduces the number of droplets and clearing up the air:

$$N_0 = \beta N_c \quad (5)$$

For woodless hilltops not too close to the ground, the interception coefficient,  $\beta$  may be considered only slightly below unity, but the coefficient drops over woods and more gently sloped areas.

Further on, we assume the average droplet diameter weighted to the average cross section,  $d_s$  to be slightly smaller value than the average volume diameter,  $d$

$$d_s = \omega d \quad (6)$$

where  $\omega$  is slightly less than 1.0.

In [7] it is shown, using Mie's theory and Beer's law, applying a technique used by Skartveit and Gjessing [13], that the visibility,  $MOR$  at a height,  $z$  within a cloud can be expressed by several parameters: The adiabatic cloud water gradient,  $\delta$  (4), the height above cloud base,  $z-h_c$ , the specific number of droplets,  $N_c$ , and the three parameters,  $\alpha$ ,  $\beta$ , and  $\omega$ ;

$$MOR(z) = f[\delta(\theta_w), (z-h_c), N_c, \alpha, \beta, \omega] \quad (7)$$

For an exposed mountain top without tall vegetation, the moist air above cloud base usually rapidly lifts, resulting in only minor droplet losses. Also assuming the cloud water to be in the liquid phase, and the droplets to form uniformly, we can use the approximation  $\alpha \approx \beta \approx \omega \approx 1$ , meaning exposed, hilly surfaces without vegetation, conditions not too close to local ground, and typically narrow droplet spectrum.

Taking  $\theta_w$  from observations, we can use (7) to calculate  $N_c$  from observations of  $MOR$  at a site at level  $z$ , and the cloud base,  $h_c$  at a representative airport station.

At a hill top Hurum, in the Oslofjord region,  $MOR$  (350m) was measured in the planning process for a new airport in the Oslo region [14]. Using cloud base observations from Rygge airport, we found  $113\ cm^{-3}$ .

So, the observations from the Hurum area suggest  $N_c = 113\ cm^{-3}$  as a climatic median value through the cold season, providing no entrainment of dryer air from above. This value then could be used at exposed sites where droplet interception may be ignorable. Since the prevailing wind direction at Hurum during low visibility comes from SSW the wind blows from the sea. Then the low clouds are dominated by sea salt nuclei feed from the sea surface. A continental contribution, however, is probable. At Gamlemsveten, a corresponding analysis is made for visibility measurements at the site and cloud height data from Vigra airport at the sea level nearby [15] resulting in  $N_c = 79\ cm^{-3}$ . Obviously, this site is of more maritime character, since it is exposed to the maritime air masses from southwest to north, while high mountains shelter against humid air from inland. So,  $N_c = 79\ cm^{-3}$  is used for

maritime air masses in the North Sea and Norwegian Sea area, while  $N_c = 113 \text{ cm}^{-3}$  may be more actual at the semi – maritime air masses in Southeastern Norway.

We know accept  $N_c = 79 \text{ cm}^{-3}$  as a typical droplet density at the maritime coasts around Norway and Scotland. Knowing the water content,  $w$  from the air temperature and the cloud base, we then can calculate the typical droplet diameter  $d$ , and all parameters which are necessary to calculate ice accretion are established.

### B. Ice Melting and Ice Shedding

Accreted ice may sublime, melt or fall off due to ice-shedding. Sundin and Makkonen, 1998 [16] presumed that ice was unloaded when the air temperature exceeded  $0^\circ\text{C}$  for at least three hours, otherwise following the method of Ahti and Makkonen [6]. Harstveit, 2002 [7] introduced an ice melt model by combining the ideas from snow cover melting [17] and energy balance at a cylinder during in-cloud icing conditions [2].

The three important terms from the energy balance model during ice melt on a cylinder are the fluxes sensible,  $Q_H$  and latent,  $Q_E$  heat transfer from the air to the melting surface, and the net radiation term  $Q_N$ :

$$Q_H = h(t_s - t_a) \quad (8)$$

$$Q_E = h \frac{\varepsilon L_e}{c_p P} (e_s - e_a) \quad (9)$$

$$Q_N = Q_{L\downarrow} - \sigma T_s^4 + Q_S(1-a) \quad (10)$$

where  $h$  is the heat transfer coefficient [2]. The water vapour term in (9) also consists of the expression,  $\varepsilon L_e / c_p P$ , where  $\varepsilon=0.622$ ,  $L_e$  is the evaporation heat,  $C_p$  the specific heat of air and  $P$  the air pressure.

The net radiation term consists of a long wave term and a short wave term. During in-cloud conditions, the long wave term,  $Q_{L\downarrow} - \sigma T_s^4$  may be written  $\sigma(T_a^4 - T_0^4)$ , Where  $\sigma$  is Stephan Boltzman constant,  $T_0=273 \text{ }^\circ\text{K}$ , and  $T_a$  ( $^\circ\text{K}$ ) is the air temperature. During clear or light cloudy conditions, the incoming part,  $Q_{L\downarrow}$ , is reduced, making the above calculation too high.

The shortwave term,  $Q_S(1-a)$ , include the incoming shortwave radiation,  $Q_S$  and the surface albedo,  $a$ . This term is difficult to handle on an iced surface in variable cloud conditions. At high latitudes, clear or light cloudy conditions at mountainous sites are dominated by negative air temperatures in the cold part of the year, where now melting is actual. In late winter and spring, and for lower latitudes through the whole winter, an attempt should be done to include short wave radiation routines in the model.

It is commonly known, that the ice loss processes frequently go faster than the ice melt model suggests, due to ice fall when reduced adhesion forces during positive temperatures dominate. Observations and calculations from Gamlemsveten [15] clearly illustrate this effect. During temperatures above  $0^\circ\text{C}$ , unloading was far faster than might be explained from a pure melt process, introducing the idea of

using a shedding factor, a factor which accelerates the ice loss during positive net energy input at the surface.

$$Q_{Meff} \approx Sh \cdot Q_M \approx Sh \cdot (Q_H + Q_E + Q_N) \quad (11)$$

## III. OBSERVATIONS AND SITE DESCRIPTIONS

### A. Brossviksåta

Brossviksåta (Fig. 1) is an exposed mountain site at the Western Coast of Norway, 723 masl, 80 km north of Bergen airport, Flesland, and 60 km south of Florø airport. There is a telecommunication mast on Brossviksåta, well known for icing on construction parts. The hilltop is well suited as a test area because it is relatively easy to visit and there is infrastructure like electricity and accommodation possibilities at the telecommunication station. Besides, the top is well exposed. There is, however, some distance to the closest airport, introducing representativeness problems when studying data from specific episodes.

On Brossviksåta, M. Drage tested out icing record methods in 2003 and 2004, and reliable ice measurements on a forced rotating vertical cylinder with 30 mm diameter were made from Feb. 24 to May 1, 2004 [18]. On Feb. 23, ice density records were made, with a result of  $500 \text{ kgm}^{-3}$ , confirming the numbers used in the model as well as recommended by ISO12494 [1]. Reliable wind measurements on the site were made in the period May 1 to Sep. 30, 2003.

We now use the work described in [18] in our model validation. Wind transfer coefficients between Flesland and Brossviksåta were first established. Flesland were chosen as input station due to the continuous 24 hours cloud data series at that station. Air temperatures were extrapolated from the airport. The distance of 80 km introduced some small inaccuracies due to missing representativity of the data. Data from Florø was used to interpret such episodes.

### B. Gamlemsveten

The mountain site, Gamlemsveten (Fig. 1) is situated at the Western Coast of Norway, 790 masl, well exposed to moist air masses from the sea. The site is situated 10 km east of Ålesund airport, Vigra. There is a telecommunication mast on Gamlemsveten, well known for icing at guy wires and other construction parts. The hilltop is very well suited as a test area because it is relatively easy to visit and there is infrastructure like electricity and accommodation possibilities at the telecommunication station. Besides, the top is well exposed, and there is an airport close to the site, meaning that representative meteorological observations exist on routine basis. Observations from Vigra show that the mountain top is well above cloud base when moist air masses stream into the area.

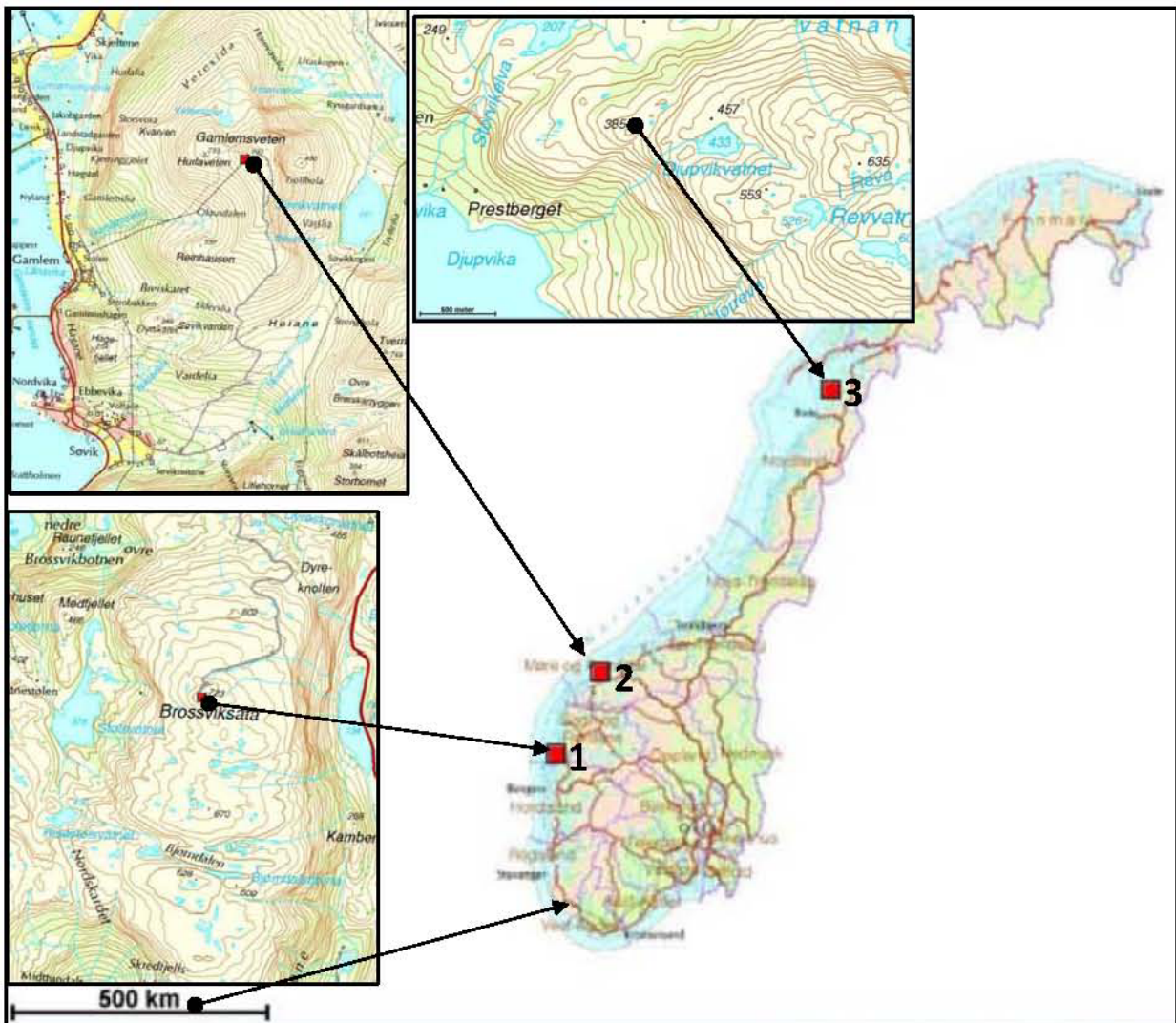


Fig. 1 Map of Norway, and the sites Brossviksåta (1), Gamlemsveten (2), and Steigen (3)



Fig. 2. Iced equipments and guy wires given by web camera pictures at Gamlemsveten.

In 2003 and 2004 a project for measuring wind under icing conditions was carried out at the site. The project was carried out by Kjeller Vindteknikk (KVT) in cooperation with Norwegian Meteorological Institute (met.no) and Institute for Energy Technology (IFE), sponsored by Norwegian Research Council, Hydro Energy (now StatoilHydro) and Statkraft, and reported at KVT [15], [19], [20].

There was mounted a 10 m mast with heated and unheated anemometer and wind vane, temperature, relative humidity, and air pressure. Besides, two Web cameras were mounted, one was viewing the instruments and the 10 m mast guy wire, and thereby the icing at an approximately vertical cylinder allowing to rotate. The other web camera was used to observe the distance to black – painted plates, distributed in given distances from the camera. Observing the visibility and knowing the cloud base from Vigra, relations may be given. Good web camera pictures exist from Feb. 2, 2004 and the rest of that winter. For the period Feb. 2 – April 27, 2004, web camera pictures as well as meteorological data from the site are available. Example of pictures is given in Fig. 2.

#### C. Steigen

There is no data from Steigen (Fig.1). However, the site was famous due to break down of the main power line to the area at Jan. 25, 2007, resulting in several villages and farms without electricity for six days in winter time. Fig. 3 illustrates the damage of the power line. Obviously, the line was covered of ice before the accident, ice pieces from the line were picked up by the workers from the power company (Nord-Salten kraftlag).

The break down was found at 385 msl. The line has performed well within a period of 15 years, though some damage due to icing at a higher level were made 15. Feb 1994, where ice observations of some 30 kg/m were made at 600 m asl.



Fig. 3. Broken power line at Steigen, 25.01.2007. Photo: Nord-Salten kraftlag

#### D. Deadwater Fell

The Deadwater Fell site (Fig. 4 - 5) is situated at a height of 580m on an isolated, exposed hill top near the Scottish/English border between the East and West coasts of the UK. It consists of a 190m test span, orientated North-South and exposed to severe winds and low clouds, and atmospheric icing during cold periods. Load cells and video cameras are mounted on a platform to measure ice loads, and a weather station is mounted nearby to monitor meteorological parameters. All the data are collected and stored at the site and down-loaded automatically via a mobile telephone to EA Technology. The data used in this investigation were kindly delivered by Brian Wareing, Tech Ltd.

The icing data were available as load data and a computer program designed for the specific power line was used to transfer the load data to ice weights.

Cloud data from several UK Met Office stations were investigated. The most suitable station turned out to be an automatic Metar station at Albemarle, 50 km east of Deadwater Fell. Due to icing on the instruments, the weather data at Deadwater were not suitable. A wind speed relation between Albemarle and Deadwater was such established through the ice – free season and used to extrapolate Albemarle data during the icing season. The temperature was extrapolated from Albemarle using the equation given in [7].

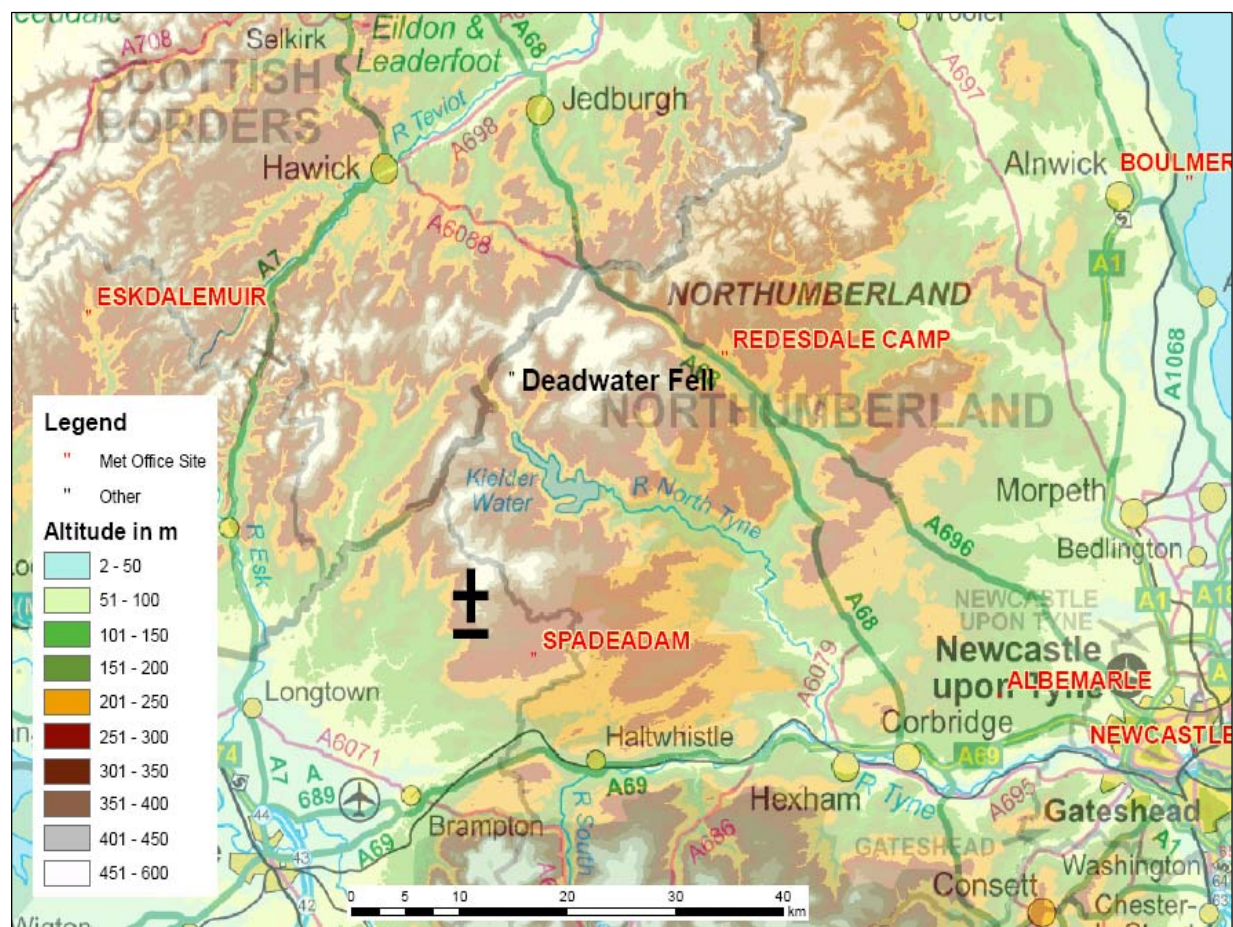


Fig. 4. The Deadwater Fell area



Fig. 5. The Deadwater Fell test station. Photo: B. Wareing

#### IV. MODELLED ICE COMPARED TO OBSERVATIONS

##### A. Brossviksåta

Observed data from Brossviksåta is shown in Fig. 6. Also shown is data modelled without shedding ( $Sh=1$ ). It is clear that at least three rapid ice losses are highly underestimated by the pure melting model. When using a shedding factor,  $Sh=10$ , a reasonable modelling is shown, while  $Sh=5$  gave too little effect. It should be emphasized that the modelled icing at March 3 is not representative due to a different cloud regime at Flesland and Brossviksåta.

From this study, the empirical ice shedding coefficient,  $Sh=10$  is included in the model. Probably, the shedding coefficient will vary within climate regions, weather situations, type of ice and type of iced objects. The coefficient is taken from the Brossviksåta case because the iced object is close to the ISO12494 – recommended object.

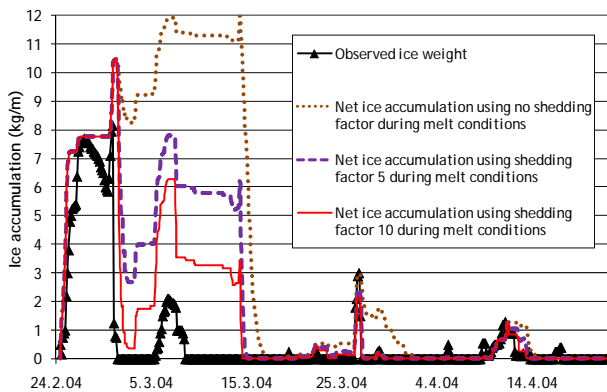


Fig. 6. Observed ice weight at Brossviksåta, Norway (723 masl) compared to modelled ice from Bergen airport data

##### B. Gamlemsveten

Ice thickness on guy wire on the 10 m mast is manually read from the web camera pictures (Fig. 2). Unfortunately, no records of ice density exists. We have therefore used  $500 \text{ kg m}^{-3}$  as a typical value suggested in [1]. When ice is formed at the windward side of the wire, it will turn, and the results will be an ice cylinder, as seen in Fig. 2. Looking away from the missing density records, the picture of the guy wire data may give similar results as a standard ISO ice collector. The lacking density measurements then enter the results as noise (possibly biased). It should be mentioned that in periods of heavy icing or very foggy weather, the camera mounted at the mast did not give readable pictures. The camera mounted at the building of the telecommunication tower, however, is more protected to ice and droplets on the lens, so we can draw some information from that camera. During the period Feb 23

- 28, the camera used for wire thickness readings was iced. However the second web camera clearly show a permanent situation where the ice on the guy wires was approximately as read at Feb 29.

For the same period as the web camera information, the ice amount is modelled using on-site temperature and wind speed data when existing, and cloud base observations from Vigra. The results are plotted in Fig. 7, where the shedding factor,  $Sh=10$  is used in the model. If  $Sh=1$  was used, the model would only remove half of the ice at Mar 1 and at Mar 2 – 16, 2004, there would be much ice left at all objects [20]. The pictures, however, showed that all ice was removed during the first six hours of Mar1. In [20] there is also concluded that there was some improvement by using temperature and wind speed measurements directly from the site, and also by using cloud droplet density information from a combined analysis of visibility records on the site and cloud base observations from the airport.

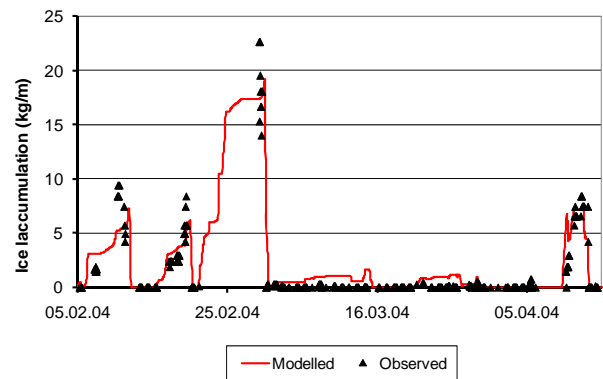


Fig. 7. Observed and modelled ice at Gamlemsveten.

##### C. Deadwater Fell

The ice weights at Deadwater Fell are small compared to the ice amounts at 700 – 800 m at the Norwegian Coast. The model clearly simulates ice weights of similar values as observed. The modelled values are close to the observed data in the season 2005/2006, but some underestimations can be seen in the 2006/2007 season. However, some deviation is to be expected due to the long distance to Albemarle (50 km). For instance, for the two situations in Dec 2006, the deviation is due to icing at temperature around  $0^\circ\text{C}$  (Dec 12), and thus very sensitive to correct temperature, or due to variations in the cloud cover in the area (Spadeadam, sited too high for regular use as input cloud data station, has cold fog around Dec 27).

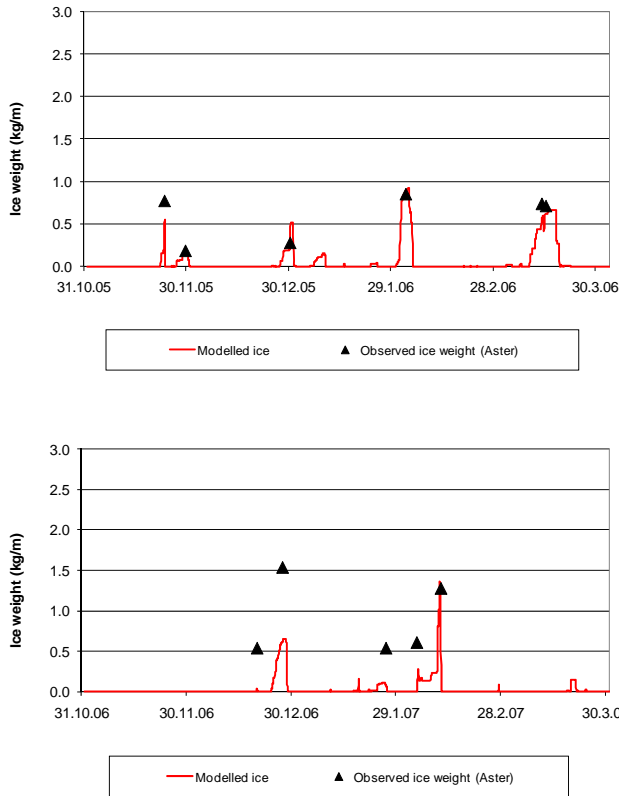


Fig. 8 Observed ice loads at the Aster test line and modelled ice at Deadwater Fell

#### D. Steigen

The modelled ice weight of 2.8 kg/m at 385 m level is a high load compared to the low height above sea level, and seems to be close to a 2 year value (data from 1996 to 2007). Combined with the wind speed of 30 m/s (10 min value) this obviously is a rare event producing high loads at the power lines and masts. The model seems to give an excellent explanation of the damage.

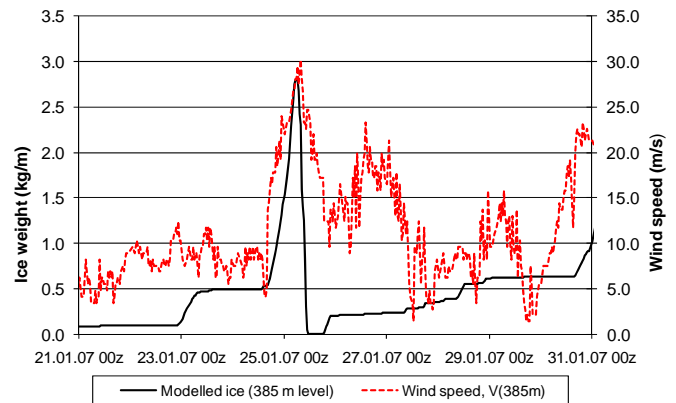


Fig. 9 Modelled ice and extrapolated wind speed in the last part of January, 2007 at Steigen, using data from Bodø airport.

## V. CONCLUSIONS

When representative and reliable cloud data, temperature data and wind data are available, in-cloud icing can be modelled at freely exposed hills in coastal regions in cold regions. Adiabatic cloud water gradients and typical values of droplet density of  $70 - 110 \text{ cm}^{-3}$  are then presumed, and collision theory as described in ISO 12494 is used. The hill should be steep enough, and free from tall vegetation to allow for fresh cloud air formed by lifting and no droplet loss to the surface.

The model give reasonable good results for sites of 10, 50 and 80 km distance between the icing site and the meteorological data source, though increasing distance means increased inaccuracy when comparing specific situations.

The model shows good strength by modelling correct ice amounts of 10 – 20 kg/m at 700 – 800 m at tops of Norwegians coastal mountains, and 1- 2 kg/m at a somewhat lower hill in UK.

When also modelling ice loss in mild weather, reasonable results are found using an accelerated energy balance model. From Brossviksåta (723 masl near Bergen) ice loss is found to be some 10 times of what can be melted using available energy from sensible, latent and radiation energy, and the same factor is suitable at Gamlemsveten (790 m near Ålesund).

## VI. ACKNOWLEDGMENTS

The Gamlemsveten data is collected with support from Statkraft, Hydro Energy, Norwegian Research Council, and Telenor. Thanks to M. Drage for using data from his dr. thesis and to Brian Wareing for data supply from Deadwater Fell.

## VII. REFERENCES

- [1] ISO/TC98/SC3/WG6, *Atmospheric icing of structures*, International Standard, ISO 12494, 2000.
- [2] L. Makkonen, «Modelling of ice accretion on wires.» *J. Climate Appl. Meteor.*, 23, 929-939, 1984.
- [3] L. Makkonen, and J. R. Stallabrass, «Experiments on the cloud droplet efficiency of cylinders.» *J. Climate Appl. Meteor.*, 26, 1406-1411, 1987.
- [4] K. Finstad, E.P. Lozowski and E.M. Gates, «A computational investigation of water droplets trajectories.» *J.Oceanic Atmos. Technol.*, 5, 160-170, 1988.
- [5] Finstad, K., E.P. Lozowski and L. Makkonen, «On the median volume diameter approximation for droplet collision efficiency, » *J.Atmos.Sci.*, 45, 4008-4012, 1988.
- [6] L. Makkonen, and K. Ahti, «Climatic mapping of ice loads based on airport weather observations, » *Atmos. Res.*, 36, 185-193.
- [7] K. Harstveit, «In-cloud rime calculations from routine meteorological observations at airfields,» in Proc. 10<sup>th</sup> Int. Workshop on Atmos. Icing of Structures, Brno, Czech Republic, 2002. Available at <http://www.vtt.fi/virtual/arcticwind/publications.htm>
- [8] A. Slingo, R. Brown and C. L. Wrench, «A field study of nocturnal stratocumulus: III High resolution radiative and microphysical observations, » *Q.J.Roy. Met.Soc.*, 108, 145-166, 1982.
- [9] V. R. Noonkester, «Droplet spectra observed in marine stratus cloud layers, » *J. Atmos. Sci.*, 41, 829-845, 1984.
- [10] P. Hignett, «A study of the short-wave radiative properties of maritime stratus: Aircraft measurements and model comparisons, » *Q. J. Roy. Met. Soc.*, 113, 1011-1024, 1987.
- [11] K. Harstveit and J. Hirvonen, «Measurements of Cloud Water Content and Droplet Density; and Calculation of Cloud Water Gradients at Kuopio, Finland.» to be presented at the 13<sup>th</sup> Int. Workshop on Atmos. Icing of Structures, Andermatt, Switzerland. 2009
- [12] R. R. Rogers, and M. K. Yau, «*A short course in cloud physics*, » Pergamon Press, 1989.
- [13] A. Skartveit, Y. Gjessing, and K. Utaaker, «Evaluating visibility and wind conditions at the Hurum hill » Meteorological Report no.1, Geophysical Institute, Meteorological Division, University of Bergen, Norway. 1990. (in Norwegian)
- [14] K. Harstveit, L. Andresen, B. Aune, M. Hansen and P.O. Kjensli, «Hurum – Weather access to an airport 290 masl.» Norwegian Meteorological Institute, Climatic Report no. 11/90, Oslo, Norway, 1990. (ISBN 0805-9918) (in Norwegian)
- [15] L. Tallhaug, K. Harstveit, and A. Fidje, «Atmospheric Icing on Wind Turbines». Kjeller Vindteknikk, KVT/LT/2005/011. Kjeller, Norway 2005 pp. 1-50
- [16] E. Sundin, and L. Makkonen, «Ice loads on a lattice tower estimated by weather station data, » *J. Appl. Meteor.*, 37, 523-529, 1998.
- [17] K. Harstveit, «Snowmelt modelling and energy exchange between the atmosphere and a melting snow cover, » Ph.D. dissertation, Scientific Report no.4, Geophysical Institute, Meteorological Division, University of Bergen, Norway. 1984:
- [18] M. Drage, «Atmospheric icing and meteorological variables – Full scale experiment and testing of models, » Ph.D. dissertation, Reports in Meteorology and Oceanography, Report No. 4, 2005, University of Bergen, Norway, 2005.
- [19] K. Harstveit, L. Tallhaug and A. Fidje, «Ice accumulation observed by use of web camera and modelled from meteorological parameters.» In the proceedings of BOREAS VII, 7 – 8. Mar 2005 (Ed. B. Tammelin et al.). Finnish Meteorological Institute, Helsinki, 2005.
- [20] K. Harstveit, L. Tallhaug and A. Fidje, «Modelling and measuring atmospheric icing at a coastal mountain in Norway, » European Wind Energy Conference, EWEC, London, 22-25. Nov 2004.